In vivo quantification of photosensitizer concentration using fluorescence differential path-length spectroscopy

de Visscher, Sebastiaan A. H. J.; Witjes, Max J. H.; Kascakova, Slavka; Sterenborg, Henricus J. C. M.; Robinson, Dominic J.; Roodenburg, Jan L. N.; Amelink, Arjen

Published in:
Journal of Biomedical Optics

DOI:
10.1117/1.JBO.17.6.067001

Publication date:
2012

Journal of Biomedical Optics

SPIEDigitalLibrary.org/jbo

In vivo quantification of photosensitizer concentration using fluorescence differential path-length spectroscopy: influence of photosensitizer formulation and tissue location

Sebastiaan A. H. J. de Visscher
Max J. H. Witjes
Slávka Kaščáková
Henricus J. C. M. Sterenborg
Dominic J. Robinson
Jan L. N. Roodenburg
Arjen Amelink

In vivo quantification of photosensitizer concentration using fluorescence differential path-length spectroscopy: influence of photosensitizer formulation and tissue location

Sebastiaan A. H. J. de Visscher,[a] Max J. H. Witjes,[a] Slávka Kaščáková,[b] Henricus J. C. M. Sterenborg,[b] Dominic J. Robinson,[b] Jan L. N. Roodenburg,[a] and Arjen Amelink[a,b]
[a]University Medical Center Groningen, Department of Oral and Maxillofacial Surgery, Division of Oncology, The Netherlands
[b]Erasmus Medical Center, Center for Optical Diagnostics and Therapy, Department of Radiation Oncology, Rotterdam, The Netherlands

Abstract. *In vivo* measurement of photosensitizer concentrations may optimize clinical photodynamic therapy (PDT). Fluorescence differential path-length spectroscopy (FDPS) is a non-invasive optical technique that has been shown to accurately quantify the concentration of Foscan® in rat liver. As a next step towards clinical translation, the effect of two liposomal formulations of mTHPC, Fospeg® and Foslip®, on FDPS response was investigated. Furthermore, FDPS was evaluated in target organs for head-and-neck PDT. Fifty-four healthy rats were intravenously injected with one of the three formulations of mTHPC at 0.15 mg kg^{-1}. FDPS was performed on liver, tongue, and lip. The mTHPC concentrations estimated using FDPS were correlated with the results of the subsequent harvested and chemically extracted organs. An excellent goodness of fit (R^2) between FDPS and extraction was found for all formulations in the liver ($R^2 = 0.79$). A much lower R^2 between FDPS and extraction was found in lip ($R^2 = 0.46$) and tongue ($R^2 = 0.10$). The lower performance in lip and in particular tongue was mainly attributed to the more layered anatomical structure, which influences scattering properties and photosensitizer distribution. [DOI: 10.1117/1.JBO.17.6.067001]

Keywords: fluorescence; meso-tetra(hydroxyphenyl) chlorin; photodynamic therapy; spectroscopy.

Paper 12031 received Jan. 13, 2012; revised manuscript received Mar. 15, 2012; accepted for publication Apr. 10, 2012; published online Jun. 4, 2012.

1 Introduction

Photodynamic therapy (PDT) has been established as a local treatment modality for several kinds of malignancies in various organs.[1–7] PDT is based on the use of a light sensitive drug, a photosensitizer, which is locally applied or systemically administered. The photosensitizer *meta*-tetra(hydroxyphenyl)chlorin (mTHPC or Temoporfin) is one of the most potent clinically used photosensitizers to date.[8–10] Its development, study and clinical use was recently summarized in a comprehensive review.[11] The formulation of mTHPC in ethanol and propylene glycol, Foscan®, is in use for both curative and palliative treatment of head and neck squamous cell carcinoma (SCC).[7,12] The treatment involves excitation of the administered photosensitizer with non-thermal light at the tumor site, which leads to the formation of cytotoxic reactive oxygen species.[9,13–17] The amount of reactive oxygen species formed depends on the type of photosensitizer, its concentration, tissue oxygenation, and the rate of irradiation. In head & neck tumors, treatment is typically performed using a mTHPC dose of 0.15 mg kg^{-1} and light fluence of 20 J cm^{-2} at a fluence rate of 100 mW cm^{-2} delivered at 652 nm.[11] However, despite the fixed light fluence and administered drug dose differences in PDT response may occur. Monitoring PDT parameters such as oxygenation, light fluence, and photosensitizer concentration during therapy could provide insight in the complex and dynamic interactions that occur during PDT and could give information on the deposited PDT dose.[18] Our group recently developed fluorescence differential path-length spectroscopy (FDPS) as a tool to quantify photosensitizer concentration and micro vascular oxygen saturation, a surrogate marker of tissue oxygen concentration.[19,20] In previous research, we were able to show that FDPS can be used to measure photosensitizer concentration *in vivo* in rat liver.[21] In this proof-of-concept study, our group used Foscan at 0.3 mg kg^{-1} as the target photosensitizer. A good linear correlation was found between the mTHPC concentration measured with FDPS and the mTHPC concentration measured by chemical extraction. As a next step towards clinical translation of FDPS for monitoring PDT in head and neck tumors, we here evaluate the performance of FDPS using a clinically relevant drug dose of 0.15 mg kg^{-1} in target organs for head-and-neck PDT: the lip and the tongue. From a tissue optics point of view it is more challenging to analyze oral mucosal tissues compared to liver tissue. For example, oral tissues such as the dorsum of the tongue and palate are keratinized and are effectively layered media, while the inner lip and floor of the mouth are less so. The keratinisation of the dorsal tongue is present in all mammals, although the degree of keratinisation varies among species.[22] In the present study, we have investigated how accurately FDPS measures photosensitizer concentrations in these more optically heterogeneous media. Similar to our previous proof-of-concept study, chemical extraction will serve as the gold standard for mTHPC concentration in these tissues.

One of the problems of Foscan in pre-clinical and clinical PDT is its poor water solubility, which results in aggregation.[11,23] Therefore, water soluble liposomal formulations have

Address all correspondence to: Sebastiaan A. H. J. de Visscher, University Medical Center Groningen, Department of Oral and Maxillofacial Surgery, Room S3.214, Hanzeplein 1, P.O. Box 30.001, 9700 RB Groningen, The Netherlands. Tel: +31 50 361 3846; Fax: +31 50 361 1136; E-mail: s.a.h.j.de.visscher@umcg.nl

0091-3286/2012/$25.00 © 2012 SPIE

been designed as nanocarriers for mTHPC. A further advantage of liposomal drug-carrier systems is a reduced uptake by the reticuloendothelial system (RES) and an enhanced permeability and retention effect (EPR).[24] Two liposomal mTHPC formulations that have been developed are Foslip® and Fospeg®.[8,25–32] In Fospeg, the surfaces of the liposomes are coated by a hydrophilic polymer to further decrease recognition by the RES and thus increase circulation time over Foscan and Foslip.[24,33] Both the incorporation of mTHPC into liposomes and the composition of different liposomes are known to significantly influence the spectral properties.[28,30] Furthermore, Foslip and Fospeg are known to exhibit different redistribution patterns and liposomal stability in serum.[30] We have therefore also investigated the influence of these nanocarriers on FDPS performance.

2 Material and Methods

2.1 *Animal and Procedures*

Fifty-four male Wistar rats (HsdCpb:W) weighing between 250 and 350 g, were purchased from Harlan Netherlands B.V. (Horst, The Netherlands). Three different formulations of mTHPC were kindly provided by Biolitec AG (Jena, Germany); Foscan® (4 mg mL^{-1} mTHPC), Fospeg® (1.5 mg mL^{-1} mTHPC) and Foslip® (1.38 mg mL^{-1} mTHPC). Prior to the experiment, Foscan, Foslip and Fospeg were dissolved for intravenous injection under minimal light and kept at 4 °C in the dark, as recommended by the manufacturer. The dosage used was 0.15 mg kg^{-1} mTHPC and animals were kept under reduced light conditions (<60 lux). Prior to the experimental measurements the rats were anaesthetized using Isoflurane®/O_2/N_2O as a general inhalation anesthetic. Variations in mTHPC concentrations are achieved by taking measurements at different time points in the pharmacokinetics profile of each formulation. At 2, 4, 8, 24, 48, or 96 h after injection ($n = 3$ animals per formulation per time point) tissue concentrations of mTHPC were measured using FDPS. In the oral cavity, four measurements were performed on the mucosa of the lip and six on the dorsum of the tongue, all at randomly chosen locations. Next, tissue overlying the liver was dissected which allowed measurements at six randomly chosen locations on the liver. Directly after the optical measurements the animals were terminated by cervical dislocation. Lip, tongue and liver were immediately excised and snap-frozen in liquid nitrogen. FDPS measured the concentration of mTHPC in lip, tongue and liver based on the emitted fluorescence of mTHPC. The concentration estimates determined by FDPS were compared to the concentration determined by chemical extraction. The experimental design for this study was approved by the experimental welfare committee of the University Medical Center Groningen and conformed to Dutch and European regulations for animal experimentation.

2.2 *Measurement of mTHPC Tissue Concentration using FDPS*

The measurement setup used, shown in Fig. 1, was based on the setup described by the group of Amelink et al.[19,21] In short, the measurement probe contained two 800 μm fibers at a core-to-core distance of 880 μm. The surface of the probe was polished under an angle of 15 deg to minimize specular reflections during the measurements. One 800 μm fiber, the delivery-and-collection fiber (dc), is coupled to a bifurcated 400 μm fiber, containing a "delivery" and a "collection" leg. The delivery leg is coupled to a 200 μm bifurcated fiber, one leg of which is connected to a xenon light source (HPX-2000, Ocean Optics, Duiven, The Netherlands) and the other leg is connected to a 405 nm diode laser (Power Technology Inc., Arkansas, USA). The collection leg is coupled to another bifurcated 200 μm fiber, of which one leg directly leads to the first channel of spectrograph setup (MC-2000-4-TR2, Ocean Optics, Duiven, The Netherlands), while the other leg leads to a 570 nm long-pass filter before leading into the second channel of the spectrograph. The second 800 μm fiber of the probe, the collection fiber (c), is coupled to a bifurcated 400 μm fiber. One leg is directly coupled to the third channel of the spectrograph, while the other leg leads to the 570 nm long-pass filter, before being coupled in to the fourth channel of the spectrograph.

Before every measurement, the FDPS system was calibrated as described previously.[7,19] The measured DPS spectra were fitted to a model extensively described by our group in the literature,[20,21,34–36] which returned quantitative estimates of blood volume fraction, micro-vascular blood oxygenation, and vessel diameter. The measured FDPS spectra are corrected for the effect of absorption by multiplying it by the ratio of DPS-signals at the excitation wavelength without and with absorption present, resulting in absorption-corrected FDPS spectra.[37] The contribution of mTHPC to the spectra was extracted by using a singular value decomposition (SVD) algorithm[38,39] using autofluorescence, Protoporphyrin IX (PpIX), and mTHPC fluorescence as basis spectra.

2.3 *Measurement of mTHPC Tissue Concentration using Chemical Extraction*

To determine the concentration of mTHPC in the excised frozen tissues, the chemical extraction method of Kascakova was used[40] on small tissue samples (~0.1 g) of lip, dorsum of the tongue, and liver. In liver it was possible to randomly obtain three samples of liver tissue per animal, representative of tissue located on the liver surface as measured by FDPS. This way, we could average multiple random locations in both optical and chemical concentrations measurements of the liver. In tongue and lip however, we could only obtain one macroscopically representative tissue sample as measured by FDPS, due to the small size of the lip and tongue of rats. All tissue samples obtained were dissolved in 2 mL of the tissue solvent Solvable™ (Perkin Elmer, Groningen, The Netherlands) over 2 h at 50°C with regular stirring. Subsequently, the solubilised solution was diluted further with Solvable™ to an optical density (OD) <0.1. The diluted samples were analyzed in a fluorimeter (Perkin Elmer, Groningen, The Netherlands) by using an excitation wavelength of 423 nm and a spectral detection band of 450 to 800 nm with a resolution of 0.5 nm. The basis spectrum of mTHPC was derived after correction for Solvable™ and autofluorescence components. The concentration of mTHPC was derived from a known calibration curve.[40]

2.4 *Statistics and Correlation*

Confidence intervals on the individual parameters for the individual measurements were determined based on the covariance matrix generated for each fit as described by Amelink et al.[41] Differences in fluorescence intensities between formulations

and tissue types at similar time points, were determined using one-way ANOVA (two-tailed) with the Bonferroni test for selected pairs of columns. Non-linear regression was used to fit a straight line forced through the origin to characterize the relation between FDPS and chemical extraction for different locations and formulations. To quantify goodness of fit of the regression lines, R^2 values and 95% confidence intervals (CI) were determined.

Differences in slope of regression lines between datasets were assessed by the sum-of-squares F-test using a confidence interval of $p = 0.05$. Pearson's correlation coefficient was used (two-tailed, 95% CI) in determining the correlation coefficients (r) between mTHPC fluorescence (FDPS) and blood volume (DPS). Graphpad Prism® (v5.0) was used for all statistical analysis.

2.5 *Confocal Fluorescence Microscopy*

Frozen tissue samples of control and mTHPC administered animals were handled under subdued light conditions. Liver, tongue and lip tissue sections of 50 μm were cut and mounted on Starfrost® adhesive glass slides (Menzel, Braunschwig, Germany). Fluorescence images were acquired at 10× magnification using a confocal fluorescence microscope (LSM510, Zeiss, Jena, Germany). Excitation and light collection was performed using a 405 nm laser equipped with a 505 nm long-pass detection filter combined with spectral detection between 545 and 706 nm at 10 nm intervals. Typically 5 μm optical slices were acquired from the center of each 50 μm section. Software written in LabVIEW (v7.1) was used to account for the autofluorescence component of the raw fluorescence; the intensity of resulting images was confirmed to be that attributable to mTHPC fluorescence.

3 Results

Typical DPS and FDPS spectra and their fits are shown in Fig. 1(a) and 1(b), respectively. The fitted mTHPC contributions of all 54 rats in the lip, tongue and liver at different time points based on the FDPS measurements are shown in Fig. 2(a). The actual mTHPC concentrations determined using chemical extraction are shown in Fig. 2(b).

3.1 *Comparison of FDPS Versus Extraction*

A global comparison of the FDPS and extraction graphs per tissue type in Fig. 2(a) and 2(b), shows a similar trend for both methods as a function of time. One noticeable difference is that FDPS clearly measures more mTHPC in the lip than in the tongue at all time points, whereas the mTHPC concentrations from extraction in these tissue types appear to be very similar. A comparison of mean fluorescence measured by extraction shows no difference ($p > 0.05$) between lip and tongue tissue. However, the same comparison in fluorescence signal measured by FDPS in Fig. 2(a) shows a significantly ($p < 0.0001$) higher intensity fluorescence in the lip.

To further investigate this issue, we plotted the mTHPC component of the FDPS fluorescence versus the mTHPC concentration measured by chemical extraction for each formulation and tissue location within the same rat, as shown in Fig. 3, thereby correcting for possible inter-animal differences in mTHPC uptake and intravenous administration. A linear regression line forced through the origin was used to characterize the relation between FDPS and chemical extraction for different locations and formulations.

In liver tissue, an excellent goodness of fit was found for Foscan, Foslip and Fospeg, as shown in Fig. 3(a). The six regression lines for lip and tongue tissues in Fig. 3(b) and 3(c) showed overall much lower R^2, except for Foslip in lip tissue. Pooling of data per tissue-type without discriminating for formulation-type, pictured in Fig. 3(d), clearly showed differences in goodness of fit between different tissue types. In the liver an excellent goodness of fit (R^2 of 0.79) was observed, while in lip ($R^2 = 0.46$) and in particular in tongue ($R^2 = 0.10$), goodness of fit was much lower.

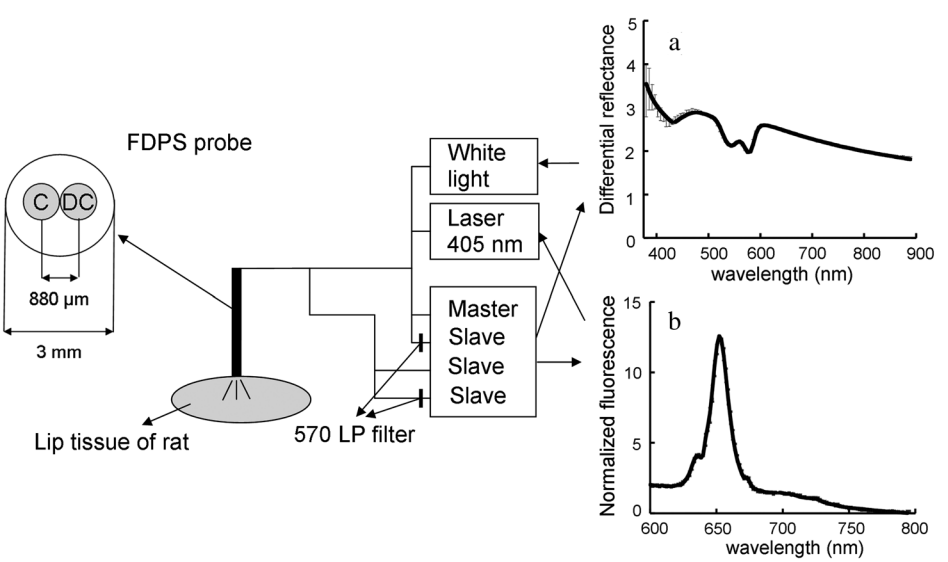

Fig. 1 Schematic diagram of the FDPS measurement setup used in our study. On the right, acquired representative paired DPS spectra and fits (a) and FDPS spectra and fits (b) from the rat lip are shown. The fluorescence spectra demonstrate both autofluorescence and fluorescence attributable to mTHPC.

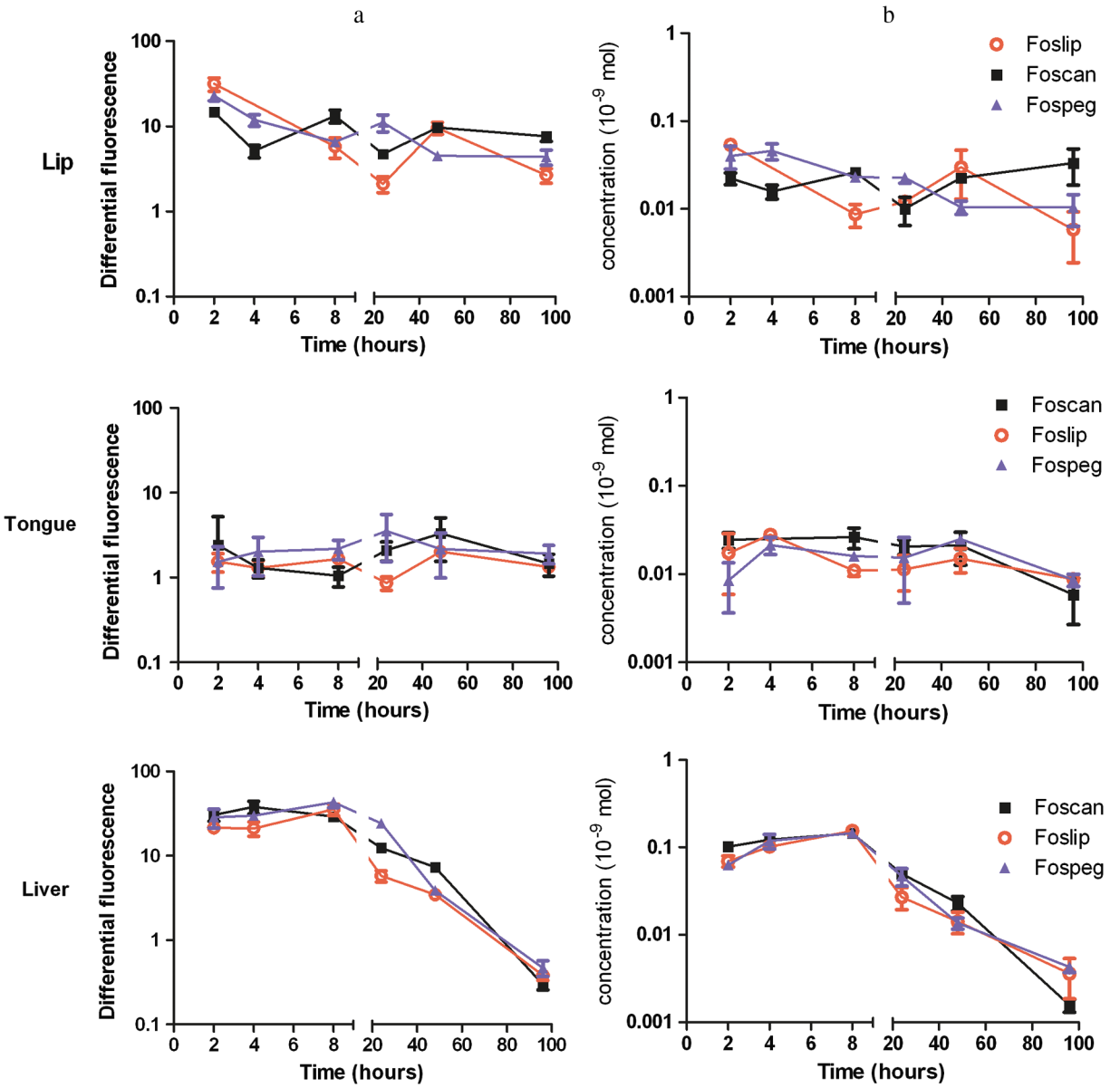

Fig. 2 mTHPC concentration vs. time measured by FDPS (a) and chemical extraction (b) in lip, tongue, and liver tissue for Foscan, Foslip, and Fospeg (error bars indicate SEM). Note the logarithmic scale used for the *y*-axes

3.2 *Influence of mTHPC Formulations and Tissue Type*

The influence of mTHPC formulation on FDPS was investigated by assessing differences in slope of regression lines within each tissue type. The sum-of-squares F-test showed a significant ($p < 0.05$, F: 3.252) difference in slope between mTHPC formulations in the liver, with Fospeg showing the highest slope in Fig. 3(a). Similar analysis in lip and tongue tissue, showed no significant ($p < 0.05$) difference in slope between the formulations. Therefore, it is possible to calculate one slope for all three formulations in tongue and lip tissue in Fig. 3(d). In lip and tongue tissue, the goodness of fit to the shared regression line (lip: $y = 388.6x$, 95% CI: 321.1 to 456.2, tongue: $y = 98.85x$, 95% CI: 80.85 to 116.9) remained similar compared to the fit to 3 individual lines. In order to assess the influence of tissue type on the slope regression lines, one overall regression line for liver was computed as well ($y = 258.4x$, 95% CI: 242.8 to 280.5). The differences in slope of the overall regression lines of liver, lip and tongue are clear in Fig. 3(d). Further statistical analysis confirmed the difference visually observed between the regression slopes of lip, tongue and liver: $p < 0.001$, F: 15.70.

To elucidate the differences between the slopes of the regression lines observed for different tissue types, the DPS data were further analyzed for scattering and blood volume fraction differences. Overall analysis of the scattering amplitude per tissue type, shown in Table 1, shows significant differences between tissue types ($p < 0.05$), with the least amount of scattering measured in the liver. No significant difference between the scattering amplitude for different mTHPC formulations was found at any time point in any tissue location. The blood volume fraction was found to have a significant correlation with mTHPC fluorescence only in the liver at the early (2, 4, and 8 h) time points; a significant Pearson's correlation (r) was found with values of 0.90, 0.57, and 0.82, respectively.

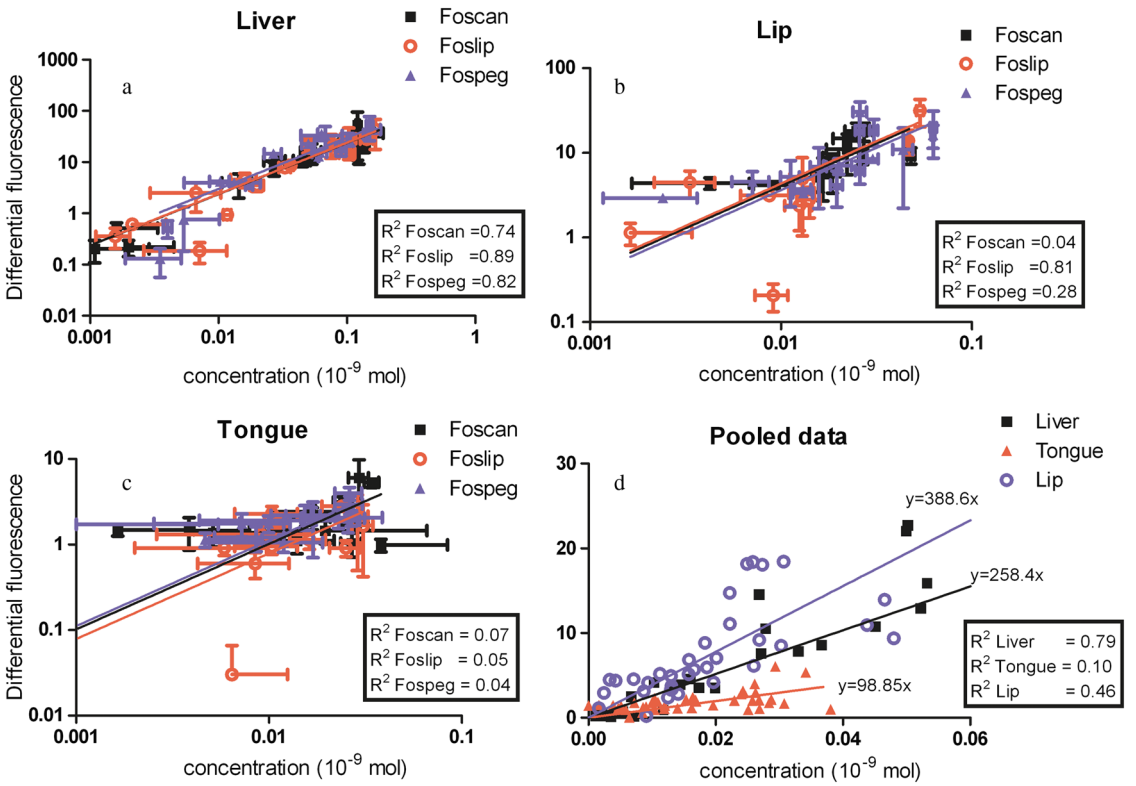

Fig. 3 Optically measured mTHPC concentration (FDPS) versus true mTHPC concentration (extraction) for 3 different mTHPC formulations (Foscan, Foslip, Fospeg) in lip (a), liver (b), and tongue (c) tissue (error bars indicate SD, logarithmic scales). One measurement point represents multiple FDPS and extraction measurements of 1 rat. Best fit linear regression lines forced through the origin are plotted as solid lines. Pooled data per tissue type (d) show significant differences ($p < 0.001$) in the slopes of the regression lines between the tissue types (linear scales). In (d), for clarity purposes only a portion of the data are shown and error bars are omitted.

Table 1 Means and standard deviations of Mie scattering amplitudes in arbitrary units measured by FDPS for different tissue types.

	Tongue	Liver	Lip
Mean	1.220	0.5579	1.722
SD	0.1150	0.01844	0.1839

3.3 *Confocal Microscopy*

To further investigate our findings of a lower correlation between FDPS and chemically extracted samples in lip and tongue versus liver, fluorescence microscopy was performed to determine differences in mTHPC distribution among tissues. Confocal fluorescence microscopy was performed on 50 μm sections of liver, tongue and lip at various time points. Typical examples are shown in Fig. 4. Differences between tissue types are clearly observable; mTHPC is homogeneously spread throughout the liver section, while in lip and especially tongue tissue mTHPC is more heterogeneously distributed. Furthermore, the presence of layered structures can be clearly seen on the transmission images in lip and especially the tongue. In tongue tissue, the filliform papillae can be clearly seen, and these structures do not contain any mTHPC. In lip tissue, a much smaller superficial layer shows no uptake of mTHPC, while an increased uptake is seen in the basement membrane.

4 Discussion

The relationship between mTHPC concentration and therapeutic outcome is complicated as numerous parameters influence the deposited PDT dose. However, the amount of mTHPC present in tissue is clearly an important factor in the PDT dosage. Non-invasive monitoring of mTHPC concentration, as well as other important parameters during PDT, could allow for standardization and optimization of clinical PDT.[4,18,42,43] The aim of this study was to test the optical photosensitizer concentration measurement technique FDPS in a more clinically relevant environment compared to previous research performed on liver tissue.[21] Therefore, in our present study we used both clinically relevant tissue locations and a clinically used drug dose. Furthermore, we tested the influence of promising new liposomal mTHPC formulations on FDPS performance.

In the liver, linear regression analysis showed an excellent goodness of fit (R^2) for the FDPS data to the extraction data, with Foscan, Foslip, and Fospeg showing similar R^2. As a further validation for FDPS with our lower drug dose we compared our R^2 to the results of Kruijt et al.[21] They found a R^2 value of 0.87 for Foscan measured by FDPS in the liver; we found a slightly lower R^2 value of 0.74. Our R^2 values were higher for Fospeg and Foslip at 0.82 and 0.89 respectively. Therefore, our measurements indicate that FDPS results could be reproduced in the liver at the clinically relevant dose of 0.15 mg/kg mTHPC, and extended to the Foslip and Fospeg formulations. Note that although the R^2 values can be compared

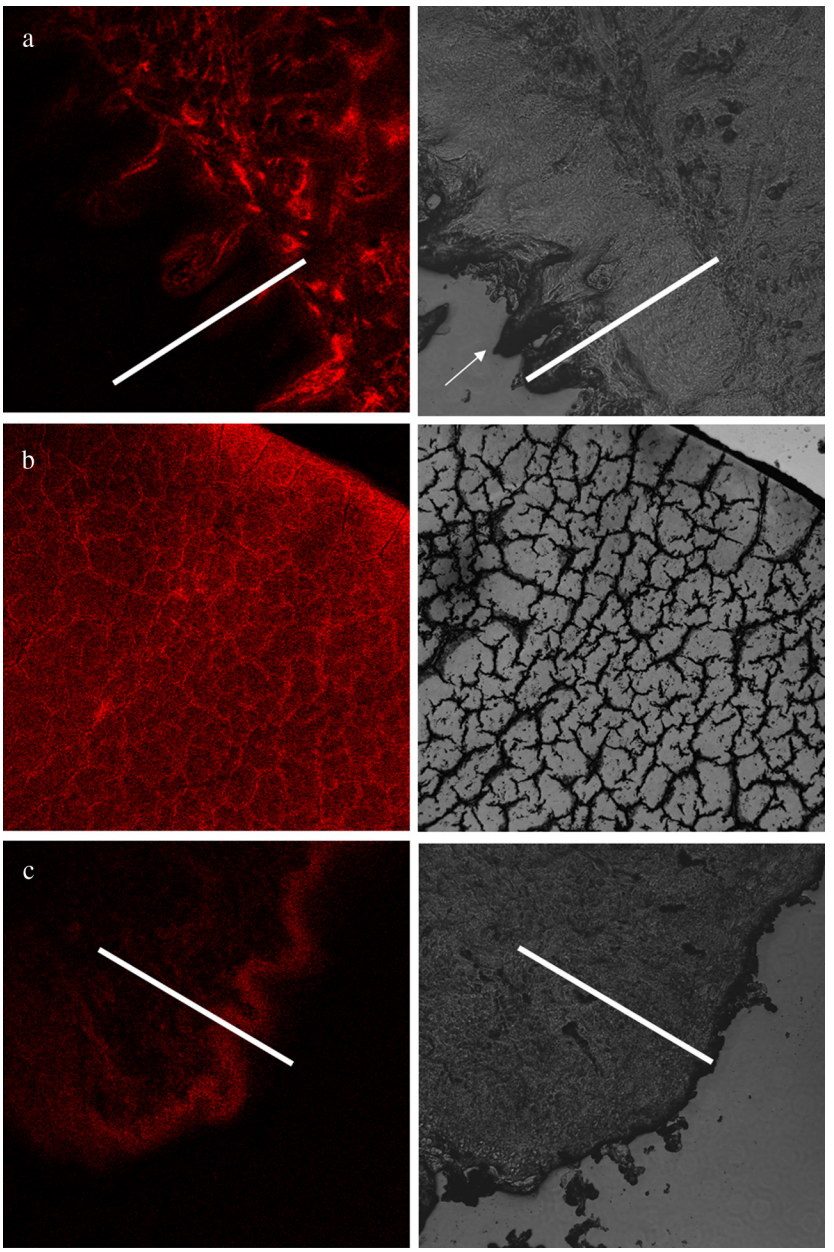

Fig. 4 Representative confocal fluorescence microscopy of tongue (a), liver (b) and lip (c). Images on the left depict distribution of mTHPC (colored red), corrected for autofluorescence. Images on the right show white light transmission images of the same slide. White scale bar: 500 μm, corresponding approximately with the interrogation depth of FDPS. The arrow in (a) indicates one of the filliform papillae on the surface of the dorsal tongue.

between this study and the study of Kruijt et al., the regression line *slopes* cannot be compared between these two studies due to differences in the distance between the probe tip and the calibration standard as well as the difference in excitation wavelengths. The shorter wavelength in the current study excites mTHPC at its maximum absorption peak, to maximize mTHPC fluorescence at a lower drug dose. Because both the calibration method and the excitation wavelength were kept constant during our current study, comparison of regression line slopes within our study is possible.

FDPS measurements in a clinically relevant and optically more demanding environment of tongue and lip tissue showed a lower correlation between the FDPS data and the extraction data. Especially in tongue tissue, the correlation was poor with R^2 approaching 0 for all formulations. FDPS in lip tissue performed only slightly better. The possible reasons for this poor correlation are discussed below.

4.1 *Influence of mTHPC Formulation on FDPS Performance*

The influence of mTHPC formulation on FDPS signal proved to be significant in liver; Fospeg showed a higher slope of the regression line compared to both Foslip and Foscan. This suggests Fospeg has a significant higher quantum yield compared to the other formulations *in vivo*. This could be explained by a relatively higher amount of non-aggregated mTHPC molecules in liposomal formulations.[24] Other *in vivo* studies also describe a higher fluorescence of Fospeg compared to Foscan,[25,26] although in these studies fluorescence intensity is

also influenced by formulation specific pharmacokinetics such as aggregation and EPR. The significant difference in slope between the regression lines of Fospeg and Foslip probably depends on the detailed characteristics of the liposomes. It is known that PEGylation of liposomes lengthens the plasma half-life of liposomes, thereby enabling a longer relative monomeric state of mTHPC in Fospeg, and resulting in a relatively higher slope of the regression line compared to Foslip.

In both tongue and lip tissue, no significant difference in slope of the regression lines between the three mTHPC formulations was present. However, this may well be related to the lower goodness of fit and the broader CI of the regression lines in tongue and lip compared to liver, making a significant difference difficult to establish.

4.2 *Influence of Tissue Type on FDPS Performance*

Data analysis in Fig. 3(d) shows very distinct differences in FDPS performance by both the goodness of fit (R^2) and the slope of the regression lines between tissue types. Fluorescence microscopy showed clear differences in the tissue-specific distribution of mTHPC at all time points; in liver, mTHPC was much more homogeneously distributed compared to both lip and tongue tissue. Furthermore, in tongue tissue an absence of mTHPC fluorescence was seen in the most superficial, dorsal layer around the papillae. In contrast, in lip tissue the distinct basement membrane close to the surface shows more mTHPC fluorescence compared to the stroma. Similar to the tongue, the most superficial layer shows almost no mTHPC fluorescence; however, in lip tissue this superficial layer of the lip is much smaller than in tongue tissue. These differences in distribution of mTHPC can be explained by the known difference in uptake of the dye in various structures like epithelium, lamina propria, striated muscle, smooth muscle, glands and fibro-connective tissue.[44–47] While liver tissue consists of multiple similar lobules, lip and tongue have a more complicated, layered composition.

The most important anatomical difference between lip and tongue tissue is the presence of keratinized stratified mucosa in the dorsal tongue while the inner side of the lip is covered by smooth non-keratinized mucosa. Besides tissue specific differences in mTHPC uptake, the biodistribution of mTHPC varies greatly with time.[46,48] However, the tissue specific mTHPC distribution is bound to have some influence on optical concentration measurements.

More challenging for our fluorescence measurement are the structural differences between tissue types. The layered, heterogeneous anatomy will certainly influence the tissue specific optical properties, in particular scattering properties. This difference is illustrated by significantly higher scattering amplitudes for lip and tongue tissue compared to liver tissue. Further indication of heterogeneity of lip and tongue tissue is given by the overall larger standard deviations of the scattering amplitude data compared to liver in Table 1.

With knowledge of the microscopic differences observed in anatomy and mTHPC distribution between tissue types, we can explain the tissue specific differences in FDPS performance.

The significant difference we found between correlation coefficients and slopes of the regression lines for different tissue types is potentially caused by a combination of three factors: 1. the layered biodistribution of photosensitizer in combination with the superficial sampling volume of FDPS *versus* the larger sampling volume of chemical extraction, 2. inter-animal variations in the thickness of the keratin layers, and 3. the large differences in scattering properties between tissue types. Although FDPS yields absorption-corrected data, it does not correct for inter- and intra-tissue scattering differences.[19,21,37] As a result, the slope of the correlation between FDPS and extraction will be influenced by the average scattering coefficient of the tissue under investigation. Table 1 shows that the scattering properties vary with tissue type, resulting in different correlation slopes; furthermore, intra- and inter-animal variations in scattering properties are more pronounced in more heterogeneous, layered tissues, such as tongue, resulting in a poorer correlation. A future challenge in improving optical concentration measurement performance would therefore be the ability to correct for scattering.[49]

With regard to the first two factors, the correlation coefficients and slopes of the regression lines are also affected by a difference in interrogation volume of both techniques (extraction and FDPS). The minimum interrogation volume necessary to obtain accurate extraction data is $\sim 10^2$ mm^3, compared to $\sim$0.2 mm^3 for FDPS. This difference will influence the slope of the regression line in tissue with a relatively heterogeneous, layered mTHPC distribution, as found in tongue and lip tissue. In tongue a large part of the FDPS interrogation volume $\sim$500 μm of the dorsal tongue consists of filliform papillae, as seen in Fig. 4. Papillae in the rat can be up to 200 μm in length[50] and showed decreased mTHPC uptake. Therefore only roughly half the FDPS interrogation volume contains mTHPC, resulting in a lower slope of the regression line between FDPS-extracted mTHPC concentration and chemical extraction in the tongue. Conversely, because the surface of the lip tissue has an increased uptake of mTHPC compared to the surface of the tongue, the FDPS-measured mTHPC fluorescence in the lip increases for the same chemically extracted mTHPC concentration. This explains the significant higher mTHPC fluorescence as measured by FDPS in lip compared to tongue tissue, whereas in the extraction the mTHPC concentrations in these tissue types appear to be very similar. Furthermore, a lower correlation will be found for tissues with more heterogeneous photosensitizer distributions. Although multiple FDPS measurements are averaged for each animal on each tissue type, inter-animal variations in photosensitizer biodistribution with tissue depth will not be averaged out and result in poor correlations. Similarly, inter-animal variations in average keratin layer thickness will also result in poor correlations between the superficially localized FDPS measurement and the "bulk" chemical extraction. The average thickness of the keratin layer in the Wistar rat tongue is described by others as 150 μm (SD $\pm$ 100), measured at a central portion of the dorsal tongue.[51] However, the highly keratinized filliform papillae are well known to have substantial, intra-animal morphological variation among differing sites of the dorsal rat tongue.[50] This is supported by the even higher variation in average thickness we found for the whole dorsal tongue; 200 μm (SD $\pm$ 120).

Extrapolation of our current results to the clinic is difficult; the dimensions and anatomy in normal human tissue are different compared to that of a rat.[52] For example, in humans the keratin layer of normal tissues is on average much smaller than in a rat, which is likely to pose less of a problem for the application of our technique on human tongue.[22,52] Furthermore, the pharmacokinetics of mTHPC differs between humans and rodents.[23] Another complicating factor is significant spatial variation in mTHPC biodistribution within tumors.[48] Moreover, tumors of

the oral cavity could also disrupt or change the keratin layer, and therefore influence the performance of our technique. All these aspects may lead to very different observations and very different levels of homogeneity and heterogeneity in human healthy and tumor tissues. In our current pre-clinical study, the emphasis has been on careful investigation of quantitative mTHPC measurements in optically more challenging tissues and of the influence of liposomal formulations. Promising nonetheless were the results of a recent clinical study using FDPS in humans.[37] The feasibility of clinical FDPS was shown, as clinical PDT treatments were monitored in three patients with SCCs of the oral cavity.

5 Conclusion

The non-invasive optical technique FDPS shows promising results in determining the mTHPC concentration in the rat liver for Foscan and for both liposomal formulations; Foslip and Fospeg. In liver, Fospeg showed a significant higher quantum yield compared to the other formulations. In optically homogeneous liver, the correlation with the chemical extraction data was excellent. In the more heterogeneous lip tissue the correlation was lower. In tongue tissue the correlation was poor. The most likely causes of these differences in correlation are the more demanding optical characteristics of lip and especially tongue tissue. In tongue tissue, FDPS performance is even further decreased by a thick layer of keratinized epithelium, which influences the optically sampled mTHPC distribution. Furthermore, in order to accurately monitor mTHPC concentration in heterogeneous tissue, a correction for scattering is needed. This is particularly important for future monitoring of mTHPC in spatially heterogeneous tumor tissues.

References

1. T. J. Dougherty, "An update on photodynamic therapy applications," *J. Clin. Laser Med. Surg.* **20**(1), 3–7 (2002).
2. S. B. Brown, E. A. Brown, and I. Walker, "The present and future role of photodynamic therapy in cancer treatment," *Lancet Oncol.* **5**(8), 497–508 (2004).
3. P. Lehmann, "Methyl aminolaevulinate-photodynamic therapy: a review of clinical trials in the treatment of actinic keratoses and nonmelanoma skin cancer," *Br. J. Dermatol.* **156**(5), 793–801 (2007).
4. B. C. Wilson and M. S. Patterson, "The physics, biophysics and technology of photodynamic therapy," *Phys. Med. Biol.* **53**(9), R61–R109 (2008).
5. C. M. Moore, D. Pendse, and M. Emberton, "Photodynamic therapy for prostate cancer—a review of current status and future promise," *Nat. Clin. Pract. Urol.* **6**(1), 18–30 (2009).
6. S. G. Bown et al., "Photodynamic therapy for cancer of the pancreas," *Gut* **50**(4), 549–557 (2002).
7. B. Karakullukcu et al., "Photodynamic therapy of early stage oral cavity and oropharynx neoplasms: an outcome analysis of 170 patients," *Eur. Arch. Otorhinolaryngol.* **268**(2), 281–288 (2011).
8. J. Berlanda et al., "Comparative in vitro study on the characteristics of different photosensitizers employed in PDT," *J. Photochem. Photobiol. B* **100**(3), 173–180 (2010).
9. T. J. Dougherty et al., "Photodynamic therapy," *J. Natl. Cancer Inst.* **90**(12), 889–905 (1998).
10. S. Mitra and T. H. Foster, "Photophysical parameters, photosensitizer retention and tissue optical properties completely account for the higher photodynamic efficacy of meso-tetra-hydroxyphenyl-chlorin vs Photofrin," *Photochem. Photobiol.* **81**(4), 849–859 (2005).
11. M. O. Senge and J. C. Brandt, "Temoporfin (Foscan(R), 5,10,15, 20-tetra(m-hydroxyphenyl)chlorin)—a second-generation photosensitizer," *Photochem. Photobiol.* **87**(6), 1240–1296 (2011).
12. A. K. D'Cruz, M. H. Robinson, and M. A. Biel, "mTHPC-mediated photodynamic therapy in patients with advanced, incurable head and neck cancer: a multicenter study of 128 patients," *Head Neck* **26**(3), 232–240 (2004).
13. B. W. Henderson and T. J. Dougherty, "How does photodynamic therapy work?," *Photochem. Photobiol.* **55**(1), 145–157 (1992).
14. V. O. Melnikova et al., "Photodynamic properties of meta-tetra(hydroxyphenyl)chlorin in human tumor cells," *Radiat. Res.* **152**(4), 428–435 (1999).
15. M. Dewaele, H. Maes, and P. Agostinis, "ROS-mediated mechanisms of autophagy stimulation and their relevance in cancer therapy," *Autophagy* **6**(7), 838–854 (2010).
16. E. Buytaert, M. Dewaele, and P. Agostinis, "Molecular effectors of multiple cell death pathways initiated by photodynamic therapy," *Biochim. Biophys. Acta* **1776**(1), 86–107 (2007).
17. M. Ochsner, "Photophysical and photobiological processes in the photodynamic therapy of tumours," *J. Photochem. Photobiol. B* **39**(1), 1–18 (1997).
18. B. C. Wilson, M. S. Patterson, and L. Lilge, "Implicit and explicit dosimetry in photodynamic therapy: a new paradigm," *Lasers Med. Sci.* **12**(3), 182–199 (1997).
19. A. Amelink et al., "Quantitative fluorescence spectroscopy in turbid media using fluorescence differential path length spectroscopy," *J. Biomed. Opt.* **13**(5), 054051 (2008).
20. A. Amelink and H. J. Sterenborg, "Measurement of the local optical properties of turbid media by differential path-length spectroscopy," *Appl. Opt.* **43**(15), 3048–3054 (2004).
21. B. Kruijt et al., "In vivo quantification of chromophore concentration using fluorescence differential path length spectroscopy," *J. Biomed. Opt.* **14**(3), 034022 (2009).
22. S. Iwasaki, "Evolution of the structure and function of the vertebrate tongue," *J. Anat.* **201**(1), 1–13 (2002).
23. M. Triesscheijn et al., "The pharmacokinetic behavior of the photosensitizer meso-tetra-hydroxyphenyl-chlorin in mice and men," *Cancer Chemother. Pharmacol.* **60**(1), 113–122 (2007).
24. A. S. Derycke and P. A. de Witte, "Liposomes for photodynamic therapy," *Adv. Drug Deliv. Rev.* **56**(1), 17–30 (2004).
25. S. A. de Visscher et al., "Fluorescence localization and kinetics of mTHPC and liposomal formulations of mTHPC in the window-chamber tumor model," *Lasers Surg. Med.* **43**(6), 528–536 (2011).
26. J. Buchholz et al., "Optimizing photodynamic therapy: in vivo pharmacokinetics of liposomal meta-(tetrahydroxyphenyl)chlorin in feline squamous cell carcinoma," *Clin. Cancer Res.* **11**(20), 7538–7544 (2005).
27. C. Compagnin et al., "Meta-tetra(hydroxyphenyl)chlorin-loaded liposomes sterically stabilised with poly(ethylene glycol) of different length and density: characterisation, in vitro cellular uptake and phototoxicity," *Photochem. Photobiol. Sci.* **10**(11), 1751–1759 (2011).
28. D. Kachatkou et al., "Unusual photoinduced response of mTHPC liposomal formulation (Foslip)," *Photochem. Photobiol.* **85**(3), 719–724 (2009).
29. T. Kiesslich et al., "Comparative characterization of the efficiency and cellular pharmacokinetics of Foscan- and Foslip-based photodynamic treatment in human biliary tract cancer cell lines," *Photochem. Photobiol. Sci.* **6**(6), 619–627 (2007).
30. V. Reshetov et al., "Redistribution of meta-tetra(hydroxyphenyl)chlorin (m-THPC) from conventional and PEGylated liposomes to biological substrates," *Photochem. Photobiol. Sci.* **10**(6), 911–919 (2011).
31. J. Svensson et al., "Tumor selectivity at short times following systemic administration of a liposomal temoporfin formulation in a murine tumor model," *Photochem. Photobiol.* **83**(5), 1211–1219 (2007).
32. M. J. Bovis et al., "Improved in vivo delivery of m-THPC via pegylated liposomes for use in photodynamic therapy," *J. Control. Release* **157**(2), 196–205 (2012).
33. B. Romberg, W. E. Hennink, and G. Storm, "Sheddable coatings for long-circulating nanoparticles," *Pharm. Res.* **25**(1), 55–71 (2008).
34. A. Amelink et al., "In vivo measurement of the local optical properties of tissue by use of differential path-length spectroscopy," *Opt. Lett.* **29**(10), 1087–1089 (2004).
35. A. Amelink et al., "Non-invasive measurement of the morphology and physiology of oral mucosa by use of optical spectroscopy," *Oral Oncol.* **44**(1), 65–71 (2008).

36. R. L. van Veen et al., "Optical biopsy of breast tissue using differential path-length spectroscopy," *Phys. Med. Biol.* **50**(11), 2573–2581 (2005).
37. B. Karakullukcu et al., "Clinical feasibility of monitoring m-THPC mediated photodynamic therapy by means of fluorescence differential path-length spectroscopy," *J. Biophoton.* **4**(10), 740–751 (2011).
38. B. Kruijt et al., "Monitoring ALA-induced PpIX photodynamic therapy in the rat esophagus using fluorescence and reflectance spectroscopy," *Photochem. Photobiol.* **84**(6), 1515–1527 (2008).
39. J. C. Finlay, S. Mitra, and T. H. Foster, "In vivo mTHPC photobleaching in normal rat skin exhibits unique irradiance-dependent features," *Photochem. Photobiol.* **75**(3), 282–288 (2002).
40. S. Kascakova et al., "Ex vivo quantification of mTHPC concentration in tissue: influence of chemical extraction on the optical properties," *J. Photochem. Photobiol. B* **91**(2–3), 99–107 (2008).
41. A. Amelink, D. J. Robinson, and H. J. Sterenborg, "Confidence intervals on fit parameters derived from optical reflectance spectroscopy measurements," *J. Biomed. Opt.* **13**(5), 054044 (2008).
42. B. Kruijt et al., "Monitoring interstitial m-THPC-PDT in vivo using fluorescence and reflectance spectroscopy" *Lasers Surg. Med.* **41**(9), 653–664 (2009).
43. D. J. Robinson et al., "Fluorescence photobleaching of ALA-induced protoporphyrin IX during photodynamic therapy of normal hairless mouse skin: the effect of light dose and irradiance and the resulting biological effect," *Photochem. Photobiol.* **67**(1), 140–149 (1998).
44. S. A. Blant et al., "Time-dependent biodistribution of tetra(m-hydroxyphenyl)chlorin and benzoporphyrin derivative monoacid ring A in the hamster model: comparative fluorescence microscopy study," *Photochem. Photobiol.* **71**(3), 333–340 (2000).
45. Q. Peng et al., "Uptake, localization, and photodynamic effect of meso-tetra(hydroxyphenyl)porphine and its corresponding chlorin in normal and tumor tissues of mice bearing mammary carcinoma," *Cancer Res.* **55**(12), 2620–2626 (1995).
46. S. Andrejevic et al., "Measurements by fluorescence microscopy of the time-dependent distribution of meso-tetra-hydroxyphenylchlorin in healthy tissues and chemically induced "early" squamous cell carcinoma of the Syrian hamster cheek pouch," *J. Photochem. Photobiol. B* **36**(2), 143–151 (1996).
47. S. A. Blant et al., "Uptake and localisation of mTHPC (Foscan) and its 14C-labelled form in normal and tumour tissues of the hamster squamous cell carcinoma model: a comparative study," *Br. J. Cancer* **87**(12), 1470–1478 (2002).
48. S. Mitra et al., "Temporally and spatially heterogeneous distribution of mTHPC in a murine tumor observed by two-color confocal fluorescence imaging and spectroscopy in a whole-mount model," *Photochem. Photobiol.* **81**(5), 1123–1130 (2005).
49. S. Kanick et al., "Semi-empirical model of the effect of scattering on single fiber fluorescence intensity measured on a turbid medium," *Biomed. Opt. Express* **3**(1), 137–152 (2012).
50. T. Nagato et al., "Three-dimensional architecture of rat lingual filiform papillae with special reference to the epithelium-connective tissue interface," *J. Anat.* **165**, 177–189 (1989).
51. A. Kobayashi et al., "Morphological and histopathological changes in tongues of experimentally developed acromegaly-like rats," *Horm. Metab. Res.* **38**(3), 146–151 (2006).
52. M. Toyoda et al., "Electron microscopic characterization of filiform papillae in the normal human tongue," *Arch. Histol. Cytol.* **61**(3), 253–268 (1998).